# Lithogenic to Organic Particle Transition Around Volcanic Saipan

Hiroki Kurihara

University of Washington

School of Oceanography, Box 357940 Seattle, WA 98195-7940

hiroki23@uw.edu

5 June 2026

**Abstract**

Suspended particle composition in coastal waters surrounding volcanic islands is expected to shift from lithogenic to organic dominance with increasing distance from shore, driven by rapid gravitational settling of terrigenous sediment on steep bathymetric slopes. This study examines the spatial extent of this transition around Saipan, a volcanic island in the oligotrophic Western Pacific, using in-situ turbidity and chlorophyll-a fluorescence measurements along two transects: a 25 km east transect originating from the largest river mouth on the island, and a 15 km west transect across the shallow insular shelf. The normalized fluorescence-to-turbidity ratio (F:T) was used as the primary indicator of particle composition. Results revealed contrasting patterns between the two transects. On the east, turbidity unexpectedly increased from 0.17 NTU in the inner shelf to 0.18 NTU in the offshore ($p << 0.01$), which is small but statistically significant, while fluorescence declined sharply within the first 3 km and remained near zero offshore, with the F:T ratio reaching near zero by the 4-8 km section - much closer to shore than the predicted 12 km transition. In the west, turbidity decreased with distance ($p << 0.01$), and the F:T ratio increased offshore, driven by turbidity decline rather than fluorescence increase. Mass concentration data supported the interpretation that the east is more lithogenically influenced, while the west is more organically influenced nearshore, as the east showed no significant turbidity-mass correlation while the west showed a stronger positive relationship ($R^2 = 0.852$). These results suggest that particle dynamics around Saipan are more spatially complex than a simple nearshore-to-offshore gradient, and that bathymetric differences between island sides play a fundamental role in controlling particle composition in oligotrophic island systems.

**Plain Language Summary**

Ocean water contains tiny particles that affect water clarity and the health of marine ecosystems like coral reefs. These particles can be either mineral sediment washed in from land, called lithogenic particles, or living and once-living organisms like phytoplankton, called organic particles. Understanding which type of particle is present matters because the same water cloudiness, or turbidity, can mean very different things depending on whether it comes from mud or from marine life. This study looked at how particle type changes with distance from shore around Saipan, a volcanic island in the Western Pacific. Water cloudiness and chlorophyll, a pigment found only in phytoplankton, were measured along two paths extending from the coast into the open ocean on the east and west sides of the island. On the east side, where the seafloor drops off very steeply, cloudiness actually increased with distance from shore, which was the opposite of what was expected, and chlorophyll dropped to near zero very close to shore. On the west side, where the seafloor is shallower and flatter, cloudiness decreased with distance as expected, but the biological signal did not follow a simple pattern and appeared to be shaped by the complex shape of the seafloor rather than by distance from shore or depth alone. Overall, particle composition around Saipan is more complicated than a straightforward nearshore-to-offshore shift, and the shape of the seafloor on each side of the island plays a big role in controlling what kinds of particles are in the water.

## 1. Introduction

In marine systems, suspended particles control water quality and light availability, affecting a wide range of marine life from coral reefs to pelagic ecosystems. These particles include lithogenic particles, which are mineral particles derived from the Earth's crust that are resistant to chemical breakdown (Ohnemus & Lam, 2015), and biogenic particles composed of phytoplankton, zooplankton, and other organic particles. Understanding the relative contributions of these particle types is critical for interpreting turbidity measurements and assessing coastal water quality, as the same turbidity value can represent many different ecological conditions depending on whether particles are primarily mineral sediment or organic particles.

Light scattering turbidity sensors work by illuminating a water sample with a light source, where photodetectors convert the light scattered from the sample to photocurrent, with the amount of photocurrent depending on the area of the illuminated particles but also on their shape, reflectivity, and other characteristics (Downing, 2006). Particle size strongly affects scattering efficiency, with smaller particles scattering more light per unit mass than larger particles, such as sand and diatom chains, due to their greater total cross-sectional area. Particle composition also matters. Lithogenic particles are typically denser with higher refractive indices and angular shapes, which means they scatter light differently than biogenic particles, which tend to be less dense, optically softer, and more irregular in shape (Downing, 2006). Mineral particles in coastal waters have lower specific scattering coefficients than organic particles in open ocean waters, primarily due to the higher density of mineral material compared to organic particles (Babin et al., 2003). Organic particles, such as phytoplankton, produce relatively more scattering per unit mass due to their lower density compared to lithogenic particles. They have lower refractive indices and higher water content than mineral particles, resulting in characteristically different backscattering signatures (Boss et al., 2001). Thus, identical readings can represent fundamentally different particle concentrations depending on particle composition. Therefore, the data must be combined or compared with other supporting measurements, such as fluorometry for chlorophyll-a concentration, to distinguish between lithogenic and organic particle sources to accurately interpret the turbidity measurements.

These sensor characteristics are particularly relevant in environments like Saipan, where particle composition is expected to shift dramatically across short distances. Saipan is a volcanic island with steep bathymetric slopes, which facilitates rapid sediment delivery to offshore waters. This creates sharp gradients in particle composition. Saipan's central volcanic ridge produces lithogenic sediment that settles quickly on the steep slope (Carruth, 2003). Although the drainage basins are small with narrow shelves, volcanic islands like Saipan have disproportionately high sediment yields relative to their basin size (Milliman & Syvitski, 1992). The island's small size limits sediment supply, so lithogenic particles cannot be efficiently transported far from shore. The eastern side of the island is exposed to open ocean conditions, with a steep insular slope that drops rapidly from the shelf edge to the abyssal plain. In contrast, the western side of the island is more sheltered with a shallow insular shelf, warmer and calmer waters, and more productive coastal ecosystems.

This combination of limited source material and rapid gravitational settling is expected to produce a sharp nearshore transition from lithogenic-dominated to mixed particle composition on the insular shelf. Because Saipan's small catchment area limits total sediment supply and the steep volcanic slope accelerates gravitational settling, lithogenic particles are expected to be largely removed from suspension before they can be transported far offshore. In contrast, particles in offshore deep waters surrounding oceanic islands are expected to be dominated by biogenic material from planktonic organisms, as terrigenous inputs diminish rapidly with distance from shore. However, high lithogenic turbidity nearshore may also restrict the production of biogenic particles by limiting light penetration for photosynthesis to occur (Kirk, 1994). As lithogenic inputs decline offshore and water clarity increases, the relative importance of biogenic particles from phytoplankton production is expected to increase, particularly in the transition zone where light availability improves but oligotrophic Western Pacific conditions limit absolute productivity (Chen et al., 2021).

While some long-term turbidity monitoring around Saipan has been conducted using satellite remote sensing, such as a study conducted by NOAA from 2002 to 2017 (NOAA, 2019), this approach does not distinguish between lithogenic and organic particle sources as it focuses on scattering of light from the ocean surface. Satellites can measure the concentration of biogenic particles, especially chlorophyll-a concentration; however, they are incapable of providing any information on lithogenic particle contributions to the turbidity. This study addresses that gap through direct in-situ measurements that combine light scattering sensing with fluorometry to quantify both total turbidity and chlorophyll particle concentrations as a proxy of organic particle concentration. Direct in-situ measurements along cross-shelf transects are therefore necessary to capture the full nearshore-to-offshore particle gradient that satellite observations cannot resolve.

This study examines the distance over which the transition from lithogenic to organic particle composition occurs in waters surrounding the volcanic island of Saipan. It is hypothesized that the east side undergoes a two-stage transition: (1) relatively rapid decline from lithogenic-dominated to mixed particles within the inner shelf (0-12 km) as sediments dilute and settle on the steep volcanic slope, and (2) gradual shift to organic-dominated waters farther offshore (12-22 km). This two-stage pattern is expected because the steep insular slope allows rapid lithogenic settling while improving light availability for phytoplankton growth, while the abyssal plain represents oligotrophic Western Pacific waters where lithogenic inputs are negligible, and biogenic particles from low-productivity planktonic communities dominate the particle pool. On the other hand, it is predicted that the west side will have no transitions, as the whole transect is in the insular shelf. Taking measurements on both sides of the island provides a broader characterization of particle dynamics around Saipan.

## 2. Methods

### 2.1 Sampling Transect on the East and West Sides of Saipan

Bathymetry data show three distinct zones on the east side of Saipan: insular shelf (0-12 km), insular slope (12-22 km), and abyssal plain (>22 km). This suggests a particle gradient from the coast to offshore. To validate this, a light scattering sensor was needed to measure particle size and concentration across a transect that fully covers these three areas to capture the predicted two-stage transition. On the other hand, the west side has a broad insular shelf with some coral reefs close to the island, indicating a much smaller particle gradient from the coast to offshore compared to the east. To collect data from all zones identified, data were collected along a 25 km transect on the east side of Saipan, from the largest river mouth on the island, to maximize the possibility of measuring lithogenic particles, as river discharge is responsible for about 90% of the lithogenic sediment in the ocean (Webb, 2023). Data was also collected on a 15 km transect on the west side.

## 2.2 In-Situ Turbidity and Fluorescence Data Collection

In-situ turbidity and fluorescence data were collected continuously along both transects using sensors attached to the flow-through system of the R/V Thomas G. Thompson. The flow-through system pumps water from the side of the hull to cool down the engines; however, many sensors are attached to the system to take measurements of water characteristics. Since this study focuses on surface water, only flow-through data are used. Although a fluorometer is already attached to the system, no sensor measures turbidity. To collect turbidity data, a tank with a turbidity sensor attached to the side was set up, and a hose from the system was inserted into the tank to continuously feed water. Measurements were taken continuously (every 10 seconds) as the ship moved along the transects (Figure 1).

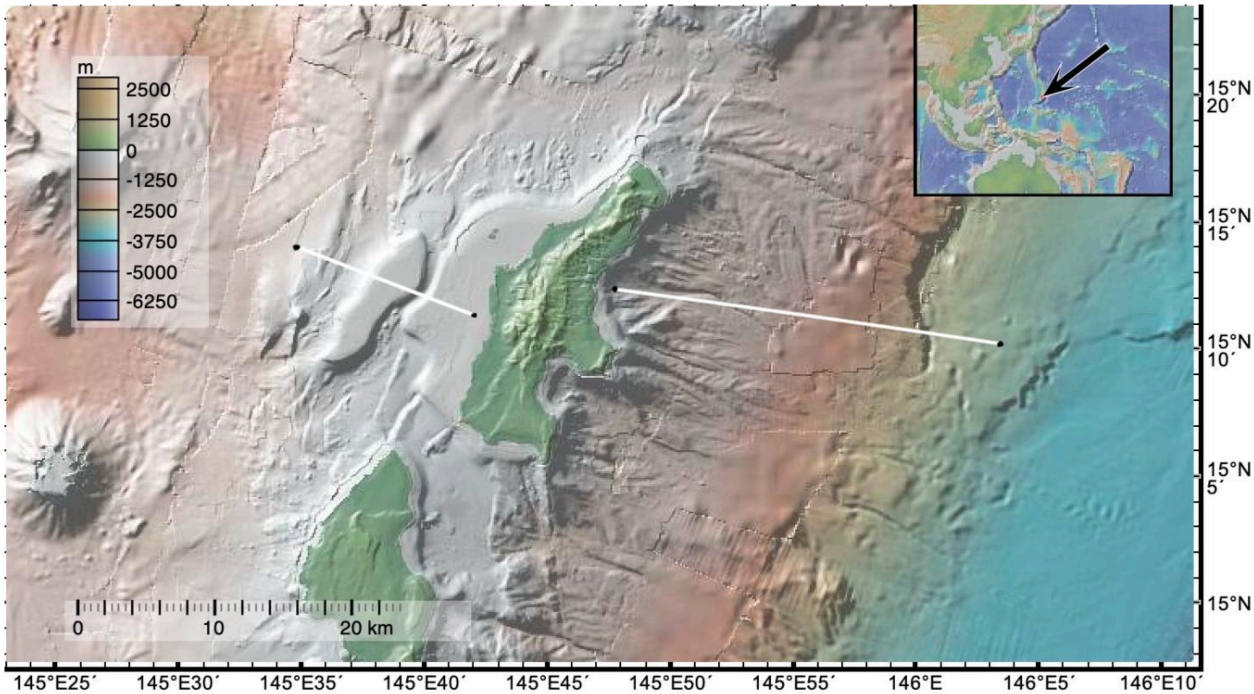


Figure 1: Sampling transects on bathymetry map. East transect: a 25 km transect extending eastward from the mouth of Saipan's largest river across the insular shelf, slope, and abyssal plain. West transect: a 15 km transect extending westward across the shallow insular shelf. Depth is indicated by the color scale shown on the top left, and a distance scale is shown on the bottom left. Data source: GeoMapApp.

The turbidity data were collected by an RBR solo light scattering turbidity sensor, and chlorophyll-a fluorescence data were collected by a shipboard WET Labs ECO FLRTD chlorophyll fluorometer attached to the flow-through system. Taking chlorophyll-a fluorescence data enables us to quantify phytoplankton biomass as a proxy for organic particle abundance. Fluorescence provides a continuous measure of phytoplankton chlorophyll; however, not all organic particles contain chlorophyll since not all are phytoplankton.

To validate the RBR solo turbidity measurements, water samples of one litre were collected every 4-5 km along each transect from the flow-through system, yielding 5 samples on the east transect and 3 on the west transect, with the larger volume chosen to ensure sufficient particle mass for analysis in these oligotrophic conditions. Filters were pre-weighed on a microbalance before the cruise. Onboard, each sample was split and filtered through pre-weighed 0.45 micron nitrocellulose filters. After returning, the loaded filters were dried and re-weighed to determine Suspended Particulate Matter concentration (SPM) in µg/L, providing a direct mass-based proxy for turbidity. SPM concentration was then plotted with respect to both turbidity and fluorescence to confirm that the sensor measurements accurately reflected actual particle concentrations. To provide regional context for the in-situ measurements, monthly composite chlorophyll-a concentration data for March 2026 were obtained from the AQUA MODIS satellite (4 km resolution) via NASA Ocean Color. This satellite data was used to characterize the broader oligotrophic background conditions surrounding Saipan rather than as a primary data source.

### 2.3 Data Processing and Visualization

The primary analytical approach was calculating the fluorescence-to-turbidity ratio (F:T) across transects. Before analysis, the F:T ratio was normalized using min-max normalization across both transects combined, scaling values to a 0-1 range using the global minimum and maximum, so that the east and west transects remain directly comparable on the same scale. Low F:T ratios indicate a relatively higher lithogenic particle contribution, and high F:T ratios a relatively lower one. The F:T ratios were plotted with respect to distance from shore to identify spatial patterns and transition zones to evaluate the relationship between them. Both fluorescence and turbidity were plotted individually with respect to distance from shore to clarify their individual pattern across the transects.

## 3. Results

### 3.1 Turbidity Patterns

The relationship between turbidity and distance from shore differed between the two transects (Figure 2, A & B). The turbidity in the east slightly changed along the transect, ranging from 0.17 Nephelometric Turbidity Units (NTU) to 0.18 NTU; however, it does not seem to have any strong relationship with distance from shore, as many points are located around 0.175 NTU. On the other hand, turbidity in the west clearly decreases as distance from shore increases, with turbidity starting at around 0.29 NTU near shore and going down to 0.19 NTU at the farthest point along the transect. Overall turbidity was also higher on the west transect, ranging from approximately 0.18 to 0.28 NTU, compared to the east, which remained around 0.17 NTU.

To quantify these patterns statistically, data were binned every 4 km from shore and summarized as boxplots (Figure 2, C & D), which confirmed the trends observed in the scatterplot with additional information on variability and outliers. On the east, although the interquartile range shifted from approximately 0.155-0.195 NTU in a 4-8 km bin to 0.16-0.19 NTU in a 20-24 km bin, most bin means remained within 0.01 NTU of each other, consistent with the pattern observed in the scatterplot. There are a large number of outliers across the transect, likely attributable to measurement artifacts such as contamination from the ship or sensor instability. In the west, the mean and interquartile range decrease with increasing distance; however, there are still many outliers with values quite far from the mean or interquartile range.

To further evaluate the predicted two-stage transition, turbidity data were divided by zone: inner shelf (0-12 km) and offshore (>12 km) for the east transect, and coastal (0-8 km) and offshore (>8 km) for the west transect (Figure 2, A & B). The plot revealed distinct differences in particle composition between regions for both transects. Although the east showed no visually obvious gradient in previous plots, the difference between the inner shelf and offshore turbidity was statistically significant ($p << 0.01$), with offshore regions having higher turbidity than the inner shelf region. The difference between regions was easier to see on the west transect, and the t-test supported it ($p << 0.01$).

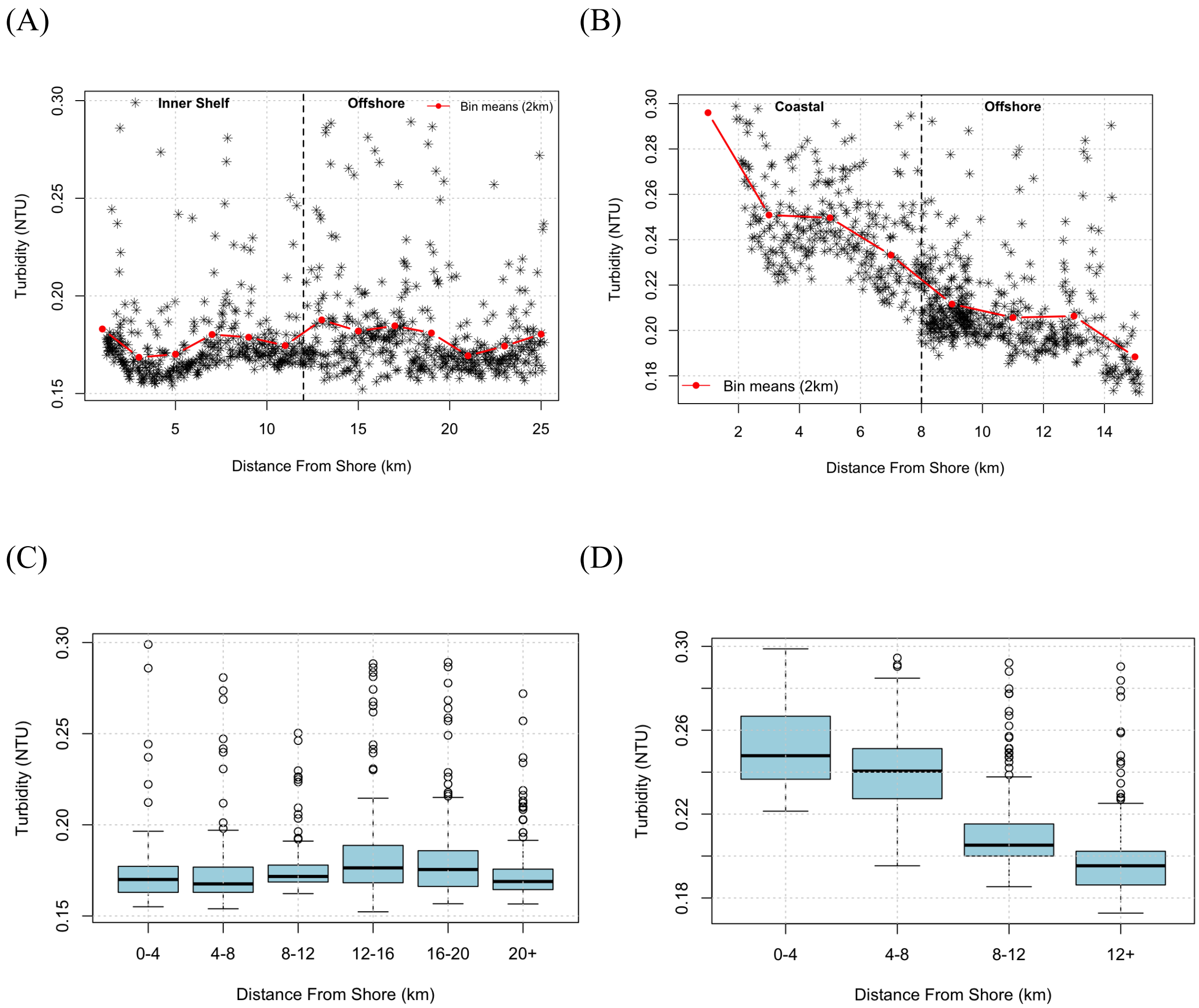


Figure 2: Turbidity (NTU) plotted against distance from shore (km) for the east transect (A, C) and west transect (B, D). (A & B): Individual measurements shown as asterisks colored by region, with filled circles representing bin means calculated every 2 km, and dashed vertical lines indicating regional boundaries. East: inner shelf (0-12 km) and offshore (>12 km), t-test $p < 0.01$. West: coastal (0-8 km) and offshore (>8 km), t-test $p << 0.01$. (C & D): Boxplots of turbidity binned every 4 km

### 3.2 Fluorescence Patterns

Fluorescence data revealed stronger and more distinct differences between the two transects than turbidity, with east ranging from 0.05 to 0.00 Relative Fluorescence Units (RFU) and west ranging from 0.13 to 0.05 RFU (Figure 3, A & B). Unlike the turbidity data, fluorescence had non-linear trends for both east and west transects with respect to distance from shore. Fluorescence decreased sharply within the first 3 km of the transect, with bin means dropping from 0.045 RFU at 0-2 km to near 0.015 RFU at 2-4 km from shore. Beyond the second point, fluorescence decreased in a very gradual slope towards the offshore. The west transect had a totally different trend. The fluorescence began at around 0.13 RFU but decreased sharply over the first 7 km, then increased again to a value close to the starting point, reaching its highest point around 11 km from shore. Beyond 11 km it decreased once more to a minimum similar in value to the low observed at 7 km. Turbidity with distance for both transects and fluorescence with respect to distance had either a near-linear correlation or a shift in one direction; however, only this data had both positive and negative slopes within the plot.

Boxplot analysis further supported the spatial patterns observed in the scatterplots (Figure 3, C & D). The biggest difference between the east and the west that could be interpreted from the boxplots is that the range of data at each section is much larger in the west than in the east. The range on the east stayed around 0.02 RFU except for the first section; however, the west showed average ranges of approximately 0.08 RFU per section compared to approximately 0.02 RFU per section on the east. Many points in the east read 0.00, which may reflect the sensor's minimum detection limit rather than a true absence of fluorescence.

Separating data by region made it clear that fluorescence in the east transect differed between the inner shelf (0-12 km) and offshore regions (>12 km) (Figure 3, A & B). Although both regions had a lot of near-zero readings, points at 0.02 RFU were less frequent in the offshore region (>12 km) than in the inner shelf region (0-12 km). This is supported statistically with a p-value of a t-test ($p << 0.01$). In contrast, the t-test confirmed that there is no statistically significant difference between the coastal region (0-8 km) and offshore region (>8 km) on the west transect ($p = 0.601$)

(A)

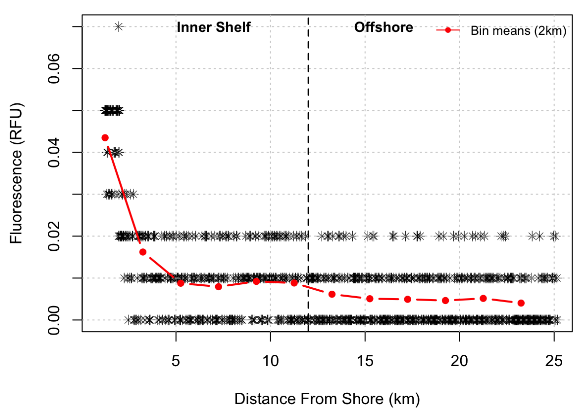


(B)

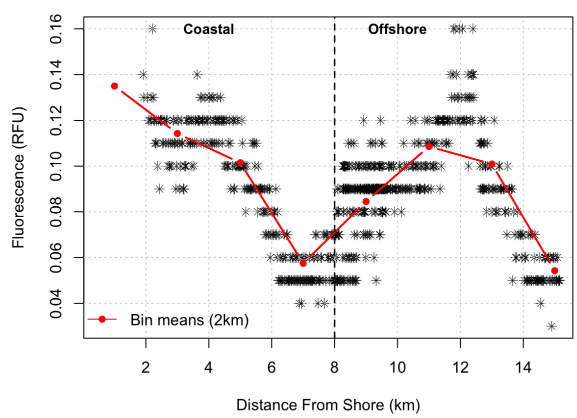


(C)

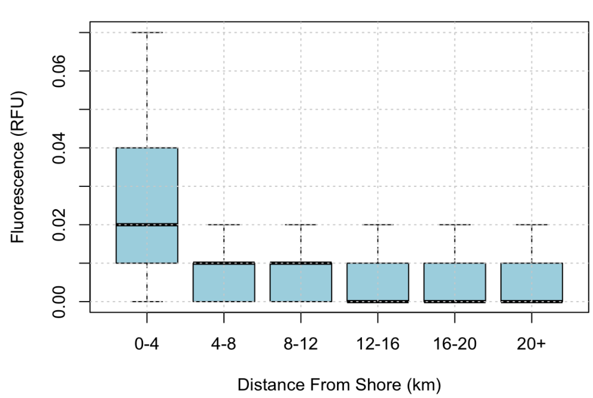


(D)

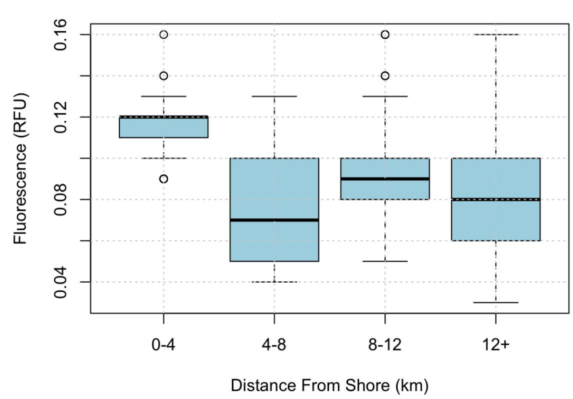

Figure 3: Fluorescence (RFU) plotted against distance from shore (km) for the east transect (A, C) and west transect (B, D). Note that the y-axis scales differ between the two transects. (A & B): Individual measurements shown as asterisks colored by region, with filled circles representing bin means calculated every 2 km, and dashed vertical lines indicating regional boundaries. East: inner shelf (0-12 km) and offshore (>12 km), t-test $p << 0.01$. West: coastal (0-8 km) and offshore (>8 km), t-test $p = 0.601$. (C & D): Boxplots of fluorescence binned every 4 km.

3.3 Relationship Between Turbidity and Fluorescence

Plotting fluorescence against turbidity reveals the relationship between these two variables across both transects (Figure 4). When both transects are plotted together, there is a statistically significant positive correlation between fluorescence and turbidity ($R^2 = 0.405$, $p << 0.01$). This suggests that higher turbidity is generally associated with higher fluorescence across the study area. However, the east and the west had completely different results when examined separately. In the east, most of the points are clustered at low fluorescence values near zero RFU across the full range of turbidity, meaning that turbidity varies considerably while fluorescence stays flat. In the west, points are located consistently higher on the fluorescence axis at similar turbidity values compared to the east. While the combined data show a positive correlation, the east and west clusters occupy clearly distinct regions of the plot, indicating that the fluorescence-turbidity relationship differs between transects.

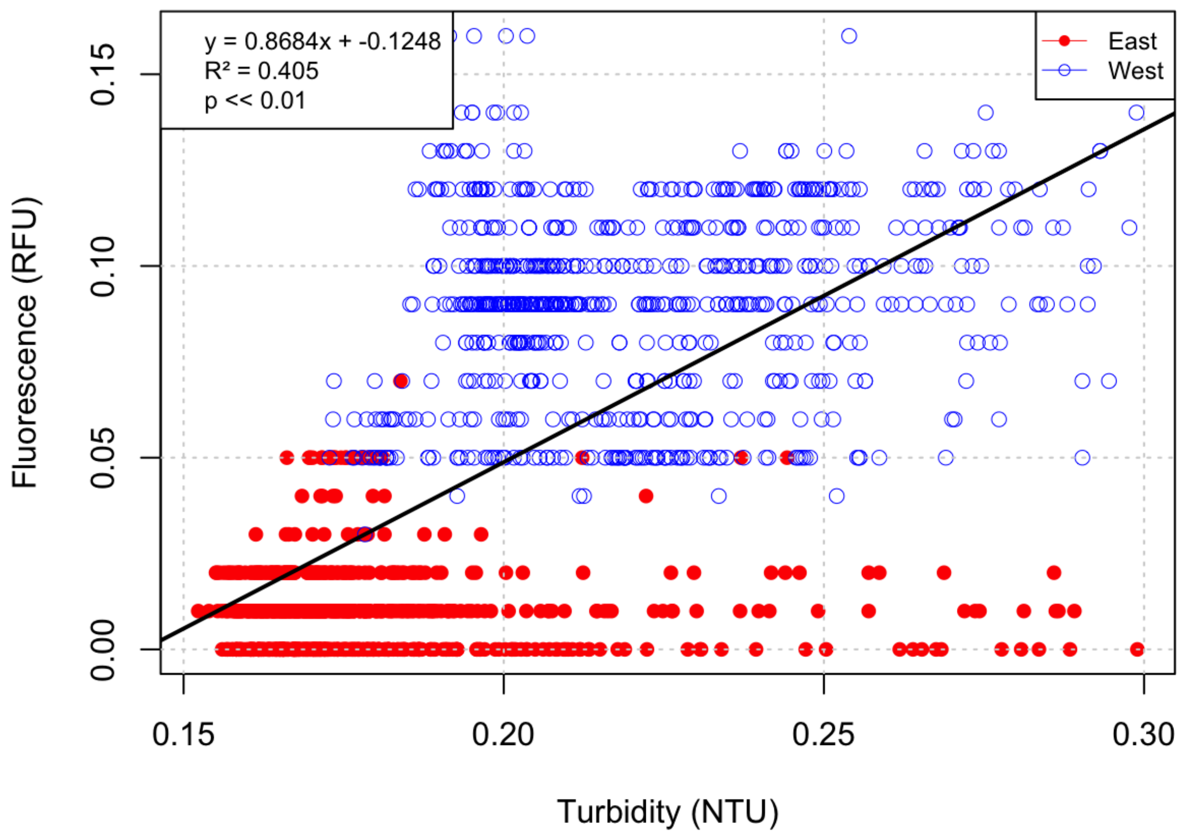


Figure 4: Fluorescence (RFU) plotted against turbidity (NTU) for both transects combined, with east transect data shown as filled circles and west transect data shown as open circles. The regression line represents the combined dataset.

3.4 Normalized Fluorescence-to-Turbidity (F:T) Ratio

The normalized F:T ratio provides the most direct test of the predicted lithogenic-to-organic transition along each transect (Figure 5, A & B). The east transect shows a ratio that decreases from a mean of around 0.18 in the 0-4 km section to near zero by the 4-8 km section, where it remains for the rest of the transect. There is no outlier in the plot, showing consistent data collection and nearly uniform overall range and interquartile range from the 4-8 km section to beyond. On the other hand, the west transect has a zigzag trend and a much larger range with a larger number of outliers - mostly on the 8-12 km section. The range is around 0.25 in the 0-4 km section, and it keeps increasing till the distance gets farther from the shore, with the 12+ km section having a range of approximately 0.65.

The ratio on the east transect decreases from the inner shelf region to the offshore region ($p << 0.01$), and both of the means are very close to 0.0, indicating consistently low F:T values across the east transect (Figure 5, C). The west transect shows a higher overall F:T ratio, increasing from the coastal region to the offshore region, with the difference also being statistically significant ($p << 0.01$) (Figure 5, D).

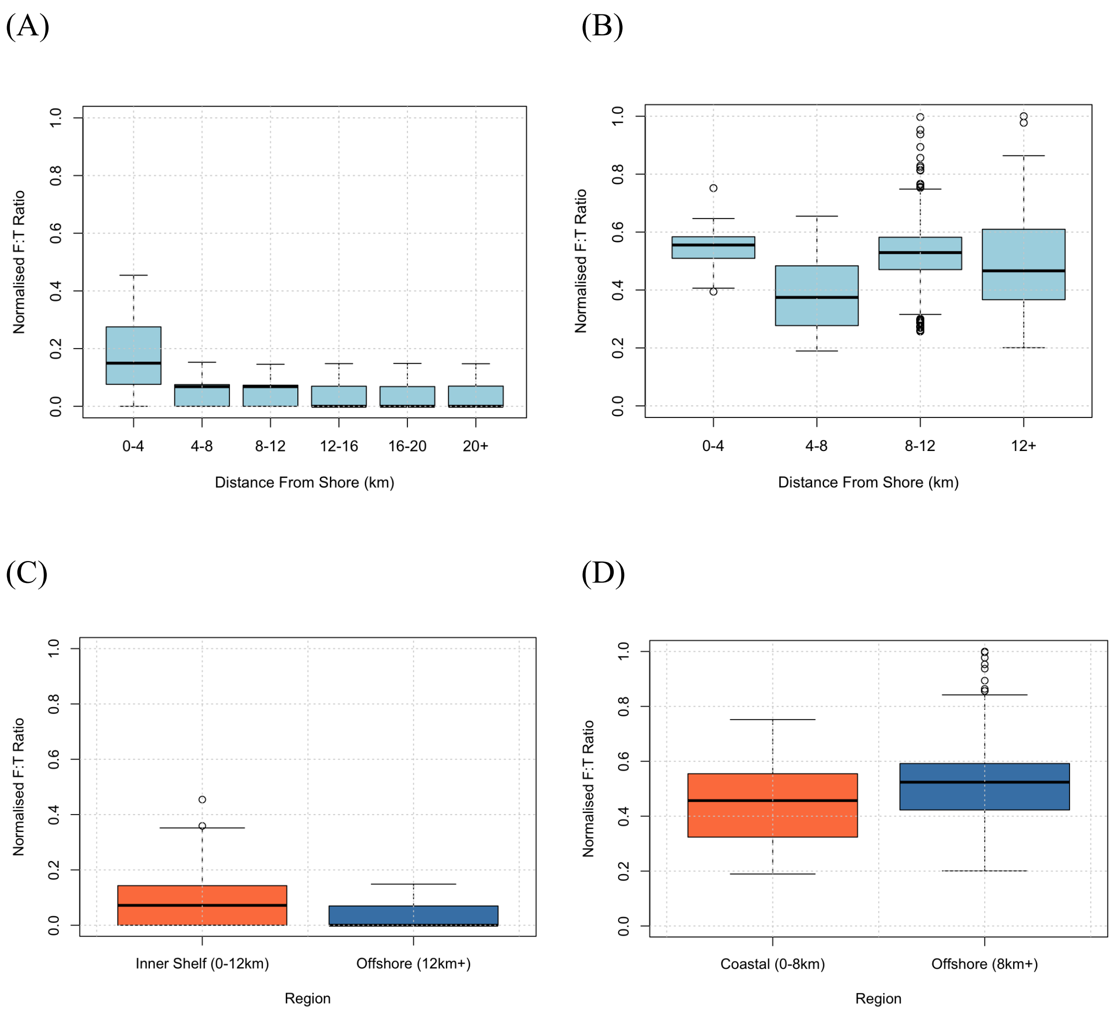


Figure 5: Normalized fluorescence-to-turbidity (F:T) ratio plotted against distance from shore (km) for the east (A, C) and west (B, D) transects. (A & B): Boxplots of F:T ratio binned every 4 km. (C & D): F:T ratio divided by region. East: inner shelf (0-12 km) vs. offshore (>12 km), t-test $p << 0.01$. West: coastal (0-8 km) vs. offshore (>8 km), t-test $p << 0.01$.

### 3.5 Validation of Sensor Data Using Water Sample Mass Concentration

Water sample mass concentration data were used to validate sensor measurements and further characterize particle composition along each transect. Turbidity showed no significant correlation with mass concentration in the east ($R^2 = 0.26$, $p = 0.380$) (Figure 6, A). The west transect showed a stronger positive relationship between turbidity and mass concentration ($R^2$ = 0.852, p = 0.251), where turbidity increased with increasing mass concentration as expected. Neither transect produced statistically significant results, likely due to the limited number of water samples collected along each transect and the low mass concentrations in all samples. Nevertheless, the relatively high $R^2$ value in the west (0.852) suggests a real positive relationship between turbidity and mass concentration that would likely reach significance with a larger sample size.

Mass concentration data provided additional support for the contrasting particle compositions between the two transects. Fluorescence showed opposite trends between the two transects when plotted against mass concentration (Figure 6, B). In the east, fluorescence decreased with increasing mass concentration ($R^2$ = 0.52, p = 0.169), suggesting that higher particle mass in the east is associated with non-fluorescent, likely lithogenic, particles rather than chlorophyll-bearing organic particles. In the west, fluorescence increased with increasing mass concentration ($R^2$ = 0.894, p = 0.211), suggesting that particle mass in the west is more closely associated with organic particles.

(A) (B)

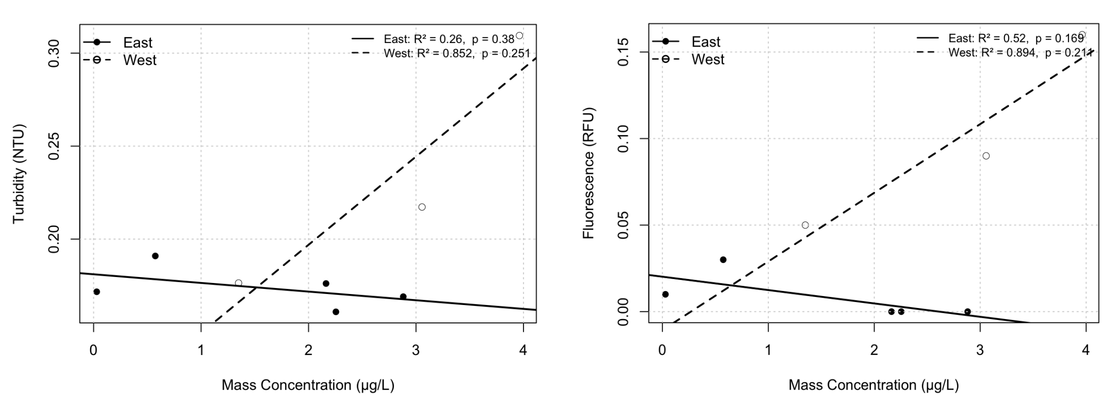

Figure 6: (A): Relationship between turbidity (NTU) and mass concentration (μg/L). East transect shown as filled circles (solid line): $R^2 = 0.26$, $p = 0.380$. West transect shown as open circles (dashed line): $R^2 = 0.852$, $p = 0.251$. (B): Relationship between fluorescence (RFU) and mass concentration (μg/L). East transect shown as filled circles (solid line), and West transect shown as open circles (dashed line).

## 4. Discussion

### 4.1 Contrasting Turbidity Patterns: East and West of Saipan

The contrasting turbidity patterns between the east and west transects reveal unexpected spatial trends that reflect the interactions between bathymetry, particle sources, and settling dynamics on each side of the island. Although the change in turbidity with distance from shore was statistically significant, the trend was positive, meaning turbidity increased with distance. This was opposite of what was predicted - it was predicted to show elevated turbidity nearshore since the transect started near the largest river mouth on the island. Visual observations from water samples suggested only minor river discharge, which may have limited the expected nearshore turbidity signal from terrestrial input. The cause might be lateral advection of particles from adjacent waters or a different offshore surface particle source; however, the specific mechanism cannot be resolved from surface measurements alone. Despite this unexpected trend, the difference was statistically significant ($p \ll 0.01$), meaning the spatial pattern is significant and not noise. In contrast, the west showed a very similar trend to what was predicted, with turbidity decreasing with distance from shore. On the east transect, turbidity showed no significant relationship with particle mass (Figure 6A; $R^2 = 0.26$, $p = 0.38$), while fluorescence decreased as mass increased (Figure 6B). Together these suggest that the particle mass on the east is largely non-fluorescent, likely lithogenic, so the turbidity signal there reflects particle composition rather than particle abundance.

## 4.2 Contrasting Fluorescence Patterns

Fluorescence patterns along both transects suggest that biological productivity is controlled by different drivers on each side of the island rather than simply by distance from shore. On the east transect, fluorescence declines sharply in the first 3 km. Although the gradient becomes more gradual, fluorescence continues to decrease with distance. The difference in values between regions is statistically significant ($p \ll 0.01$). Many data points read near zero, which may reflect the sensor's minimum detection limit rather than a true absence of fluorescence.

On the west transect, the difference was not statistically significant ($p = 0.601$), and fluorescence displayed a zig-zag trend rather than a distance-driven pattern. This suggests that on the west side, distance from shore is not the main driving factor of fluorescence. Since the west transect crosses a shallow shelf with complex morphology, including carbonate banks and channels, rather than a steep slope, changes in water column depth and local topography influence mixing dynamics and nutrient availability, which in turn affect phytoplankton distribution. To test whether depth drives this pattern, fluorescence was plotted against water depth, which ranged from approximately 0 to 900 m along the west transect (Figure 7). The relationship was not statistically significant ($R^2 = 0.001$, $p = 0.639$), indicating that water depth alone does not explain the fluorescence variability. This points to more complex drivers than a simple depth gradient: island bathymetric slope and reef area have been shown to govern phytoplankton biomass enhancement near oligotrophic islands (Gove et al., 2016), and the zig-zag fluorescence trend is consistent with spatially heterogeneous productivity driven by the banked, channeled morphology of the western shelf. As with turbidity, outliers in the fluorescence boxplots likely arise from the same collection and mounting artifacts, which probably contributed to the high variance in the 8-12 km section of the west transect.

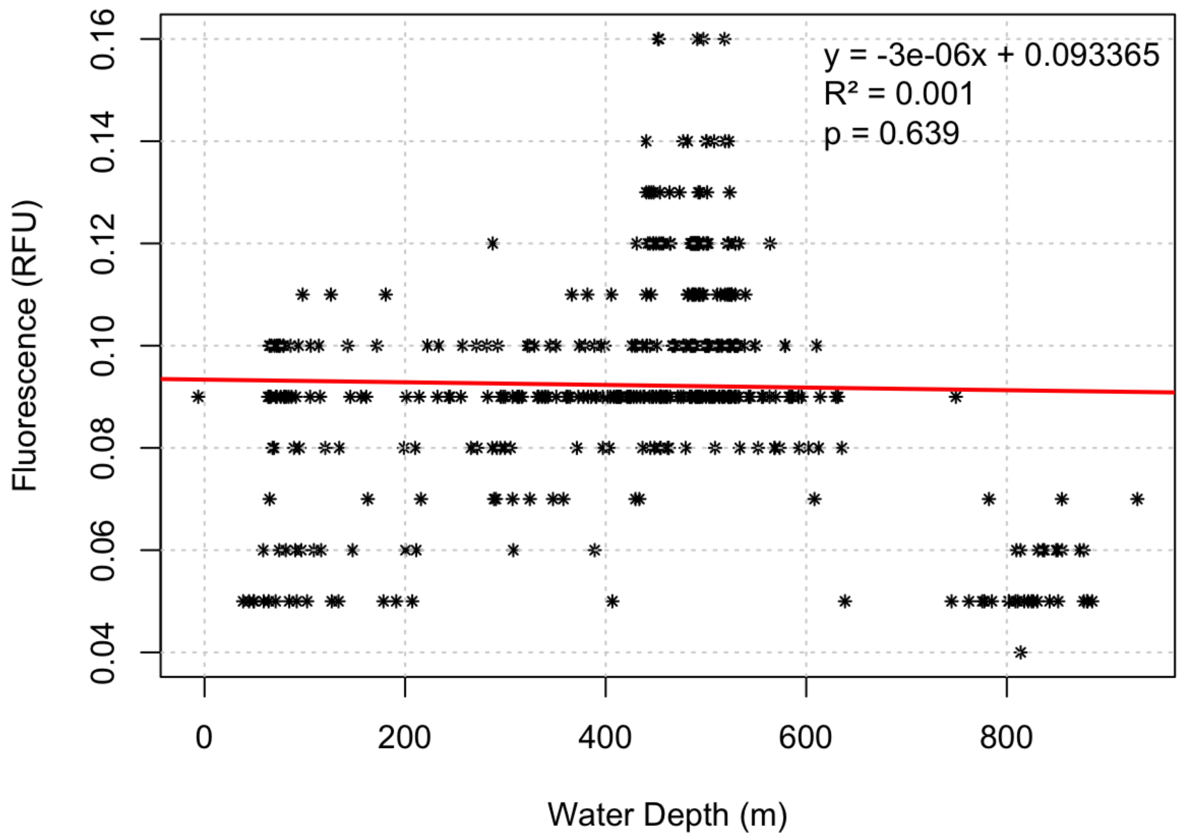


Figure 7: Fluorescence (RFU) plotted against water depth (m) along the west transect. The regression shows no significant relationship ($R^2 = 0.001$, $p = 0.639$), indicating that fluorescence is not controlled by water depth alone.

The AQUA MODIS satellite chlorophyll-a composite for March 2026 showed relatively uniform and low concentrations across the study area (Figure 8), with slightly elevated values on the west side of Saipan. This confirms that the region around Saipan Island is in clear oligotrophic conditions with no nearshore to offshore gradient, as chlorophyll concentration is uniformly low, except for the very shallow bay on the west side of the island. The satellite composite is broadly consistent with the oligotrophic conditions observed in situ; however, the satellite data did not capture the zig-zag trend in fluorescence observed along the west transect. This discrepancy is likely due to the coarse 4 km resolution of the MODIS product, which cannot resolve the fine-scale nearshore gradients captured by the in-situ sensor. Additionally, satellite retrievals are limited to the ocean surface and are susceptible to atmospheric correction errors in coastal waters, further reducing their ability to detect subtle spatial variations. This highlights the complementary value of direct in-situ measurements over satellite observations in resolving particle dynamics in nearshore oligotrophic environments.

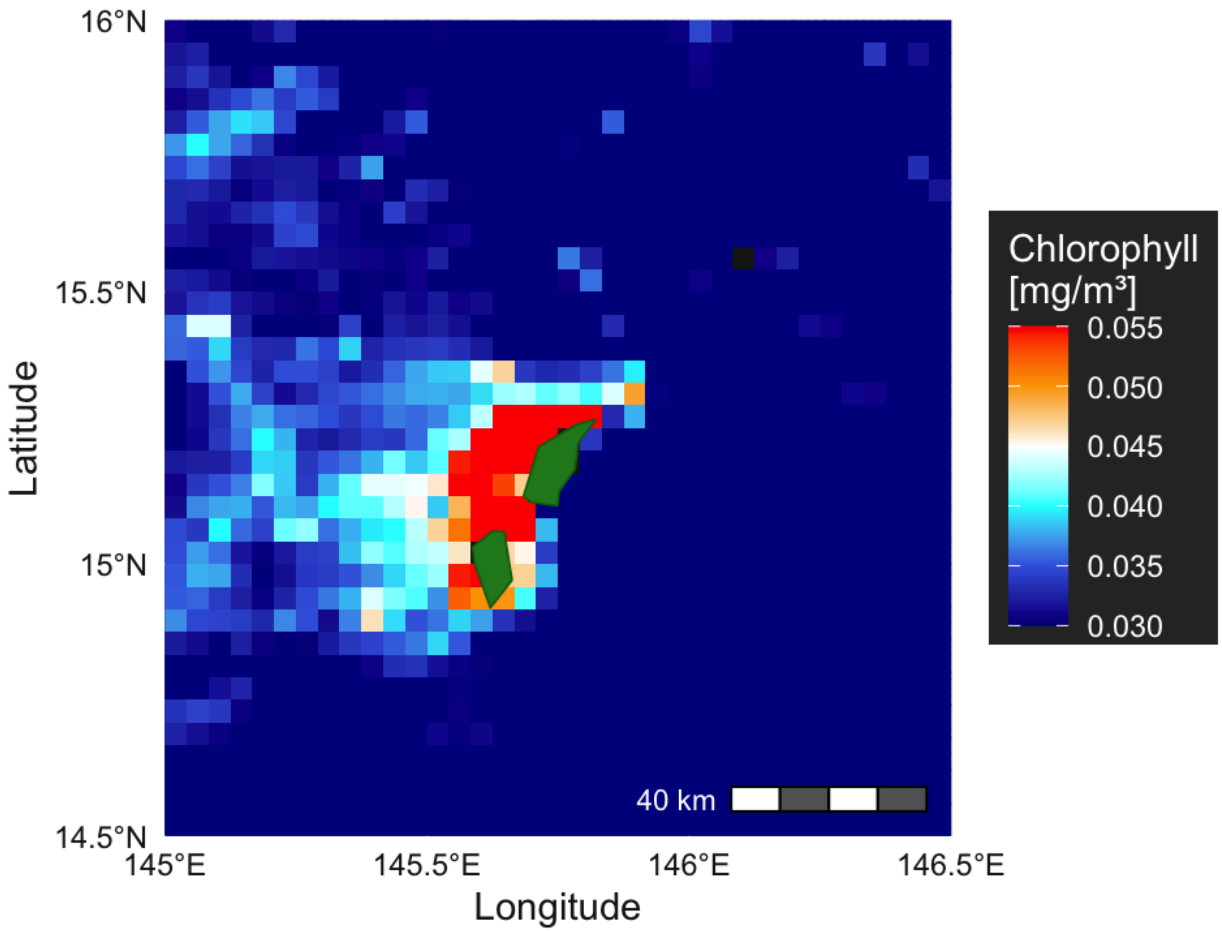


Figure 8: Monthly composite chlorophyll-a concentration (mg/m³) around Saipan for March 2026 from AQUA MODIS (4 km resolution). Saipan Island is outlined in the center of the map. Data source: NASA Ocean Color.

### 4.3 F:T Ratio as Evidence for Spatial Changes in Particle Composition

The normalized F:T ratio provides the most direct evidence for spatial changes in particle composition along each transect, though it must be interpreted carefully given the oligotrophic conditions surrounding Saipan. A low F:T ratio indicates a relatively higher lithogenic contribution, and a high F:T ratio a relatively lower one; given the oligotrophic setting, all locations remain dominated by biogenic particles. In the east transect, the ratio reached near-zero in the 4-8 km section, which contradicts the prediction of a transition at 12 km from the shore and suggests that the transition happens closer than expected. This may be because biological activity is very limited in areas other than the nearshore, as supported by the fluorescence vs distance from Figure 3. The ratio may also be an unreliable indicator in oligotrophic water, such as the waters surrounding Saipan, as both turbidity and fluorescence are very low, which could make the F:T ratio unreliable due to the minimum scale of measurement available on sensors (Downing, 2006). This limitation follows directly from the optical behavior described earlier: because lithogenic particles scatter more strongly per unit mass than the optically softer organic particles, near the sensor's detection floor the F:T ratio becomes especially sensitive to small absolute differences in either signal. Furthermore, the consistently low turbidity values across both transects suggest that lithogenic particle concentrations were very low throughout the entire study area at the time of sampling. This raises the possibility that organic particles may dominate the particle pool across both transects, with spatial differences reflecting variations in organic particle abundance rather than a true lithogenic-to-organic transition. However, direct particle composition measurements would be needed to confirm this interpretation. The west transect had a higher overall F:T ratio compared to the east, and it increased from the coastal region to the offshore region, with the difference being statistically significant ($p << 0.01$). Overall, the results partially supported the predicted lithogenic-to-organic transition on the east transect, with the shift occurring closer to shore than anticipated (4-8 km rather than 12 km). On the west transect, the hypothesis was not supported, as the increasing F:T ratio offshore was driven by turbidity decline rather than organic particle increase.

### 4.4 Limitations and Sources of Uncertainty

Several methodological and environmental factors limit the conclusions that can be drawn from this dataset and should be considered when interpreting the results. First, fluorescence only captures chlorophyll-bearing particles, so non-photosynthetic organic particles are invisible to the measurements. This likely underestimates total organic particle abundance, especially in oligotrophic waters where heterotrophic organisms can be a significant component of the particle pool (Stramski et al., 2001). Another limitation is the resolution of the sensors used. Many data points were near-zero, especially fluorescence, due to the oligotrophic water characteristics. This means that a small change or shift in values could be critical in capturing the trend; however, since the sensors have a minimum scale, this study could have missed those small trends that might have existed. Lastly, the data cleaning process introduced a limitation. Turbidity and fluorescence data collected while the ship was stationary were excluded during processing, since these sampling stops produced a great deal of noise. Removing them, however, may also have discarded real signal, so future work should log station and underway periods separately rather than deleting them, and collect additional complementary measurements, such as loss-on-ignition and particulate organic carbon, to more accurately interpret the transition between lithogenic and biogenic particle contributions.

## Conclusions

This study examined the spatial transition from lithogenic to organic particle composition in waters surrounding the volcanic island of Saipan using combined turbidity and fluorescence measurements along two contrasting transects. The east and west transects showed fundamentally different particle dynamics that reflect the contrasting bathymetry and particle sources on each side of the island. On the east transect, turbidity unexpectedly increased from the inner shelf to offshore, opposite to what was predicted. Fluorescence on the east declined sharply within the first 3 km and remained near zero for the rest of the transect. The F:T ratio reached near zero by the 4-8 km section, suggesting the lithogenic-to-organic transition occurs much closer to shore than the predicted 12 km, though the reliability of the ratio in these oligotrophic conditions is limited by sensor detection thresholds. Additionally, the consistently low turbidity across both transects suggests that organic particles may dominate the particle pool throughout the study area. On the west transect, turbidity decreased with distance as expected, and the increasing F:T ratio offshore was driven by turbidity decline rather than any increase in fluorescence, suggesting lithogenic particle dilution rather than organic particle increase. Mass concentration data further supported the interpretation that the two transects have fundamentally different particle compositions, with the east being more lithogenically influenced and the west being more organically influenced nearshore. Fluorescence on the west transect showed a zig-zag pattern more consistent with the complex bathymetric morphology of the shallow shelf than with distance from shore, suggesting that island topography influences local productivity patterns. Together, these findings suggest that particle composition around Saipan is more spatially complex than a simple nearshore-to-offshore gradient, highlighting the importance of measuring both sides of islands with contrasting bathymetric profiles to fully characterize particle dynamics in oligotrophic coastal systems.

**Acknowledgements**

First, I would like to thank the captain and crews of R/V Thomas G. Thompson for supporting my research. A huge thank you to my mentor, Dr. Andrea Ogston, for unconditional support in and out of the classroom, as well as to other teaching members of the thesis course, Dr. Ginger Armbrust, Dr. Randie Bundy, Dr. Alison Gray, and Dr. François Ribalet, for their guidance and assistance. Additionally, I would like to thank Dr. Sasha Seroy, Kendall Fontenot, and Jiaqi Li for technical support.

AI tools (Grammarly and Claude) were used to fix grammar and get suggestions on the wording and format to make the overall writing sound more professional. AI tools were also used to help create plots using R.

## References


Babin, M., A. Morel, V. Fournier-Sicre, F. Fell, and D. Stramski (2003), Light scattering properties of marine particles in coastal and open ocean waters as related to the particle mass concentration, Limnology and Oceanography, 48(2), 843–859, doi:10.4319/lo.2003.48.2.0843.

Boss, E., M. S. Twardowski, and S. Herring (2001), Shape of the particulate beam attenuation spectrum and its inversion to obtain the shape of the particulate size distribution, Applied Optics, 40(27), 4885, doi:10.1364/ao.40.004885.

Carruth, R. L. (2003), Ground-water resources of Saipan, Commonwealth of the Northern Mariana Islands, Ground-Water Resources of Saipan, Commonwealth of the Northern Mariana Islands. Available from: https://pubs.usgs.gov/wri/wri034178/htdocs/wrir03-4178.html

Chen, Z., J. Sun, T. Gu, G. Zhang, and Y. Wei (2021), Nutrient ratios driven by vertical stratification regulate phytoplankton community structure in the oligotrophic western Pacific Ocean, Ocean Science, 17(6), 1775–1789, doi:10.5194/os-17-1775-2021.

Downing, J. (2006), Twenty-five years with OBS sensors: The good, the bad, and the ugly, Continental Shelf Research, 26(17–18), 2299–2318, doi:10.1016/j.csr.2006.07.018.

Gove, J. M. et al. (2016), Near-island biological hotspots in barren ocean basins, Nature Communications, 7, 10581, doi:10.1038/ncomms10581.

Kirk, J. T. O. (1994) Light and Photosynthesis in Aquatic Ecosystems, 2nd Edition, Cambridge University Press, Cambridge.

Milliman, J. D., and J. P. Syvitski (1992), Geomorphic/tectonic control of sediment discharge to the ocean: The importance of small mountainous rivers, The Journal of Geology, 100(5), 525–544, doi:10.1086/629606.

NOAA (2019), National Oceanic and Atmospheric Administration, Department of Commerce - coastal turbidity on the shelf of the Commonwealth of the Northern Mariana Islands (CNMI) - monitoring turbid water sources and fates by satellite - Mañagaha marine conservation area, Saipan (MANM1) (NCEI accession 0204272), Catalog. Available from: https://catalog.data.gov/dataset/coastal-turbidity-on-the-shelf-of-the-commonwealth-of-the-northern-mariana-islands-cnmi-monitor6

Ohnemus, D. C., and P. J. Lam (2015), Cycling of lithogenic marine particles in the US geotraces North Atlantic transect, Deep Sea Research Part II: Topical Studies in Oceanography, 116, 283–302, doi:10.1016/j.dsr2.2014.11.019.

Stramski, D., A. Bricaud, and A. Morel (2001), Modeling the inherent optical properties of the ocean based on the detailed composition of the planktonic community, Applied Optics, 40(18), 2929–2945, doi:10.1364/AO.40.002929.

Webb, P. (2023), 12.2 lithogenous sediments, Introduction to Oceanography. Available from:

https://rwu.pressbooks.pub/webboceanography/chapter/12-2-lithogenous-sediment